*http://journal.rmutp.ac.th/*

# A Simple Solid-solid Reaction for the Synthesis of Lead Sulfide-montmorillonite Hybrid

Areeporn Baoulan[1]* and Sonchai Intachai[2]

[1] Faculty of Sciences and Liberal Arts, Rajamangala University of Technology Isan

[2] Faculty of Science, Thaksin University

[1] 744 Suranarai Road, Mueang, Nakhon Ratchasima, 30000

[2] 222 Ban Phrao, Papayom, Phatthalung, 93210

*Received 9 May 2018; Revised 16 August 2018; Accepted 29 August 2018*

## Abstract

The hybrid materials of lead sulfide with montmorillonite were synthesized by a solid-solid reaction between lead-exchanged montmorillonite and sodium sulfide at ambient condition. The hybrids were characterized by powder X-ray diffraction (XRD), thermogravimetric-differential thermal analysis (TG-DTA). The basal spacing of heat-treated lead sulfide-montmorillonite-sodium sulfide (200$^{o}$C) was 1.20 nm. The formation of lead sulfide in the hybrid confirmed by the non-resolved absorption band and absorption onset at 328 and 508 nm, respectively for heat-treated lead sulfide-montmorillonite-sodium sulfide. The dramatic blue-shifted in the absorption onset relative to that of bulk was observed.The heat treated lead sulfide-montmorillonite-sodium sulfide showed an emission peak at 367 nm. The removal of adsorbed water resulted in the increasing intensity of the hybrid.

**Keywords :** Montmorillonite; Solid-solid Reaction; Lead Sulfide; Optical Properties

**** Corresponding Author. Tel.: +669 73421394, E-mail Address: ontamareeporn@yahoo.com***

## 1. Introduction

Metal chalcogenide semiconductors (II-VI) have unique electronic and optical properties and are useful in photodetectors, optical switches, solar cells, novel nanodevices such as light-emitting diodes due to their controllable sizes and morphologies [1], [2]. Among semiconductor, lead sulfide (PbS) is an important semiconductor with a small bulk band gap (0.41 eV) and a large exciton Bohr radius of 18 nm [3]. PbS nanoclusters have attracted considerable interest due to their luminescence characteristics with the unique emission bands dependent upon the physical dimensions and the matrix, leading to great applications potential in the nanoscale lasers, light emitting diodes, solar cells and biosensors [4], [5]. Various synthetic routes have been developed in the synthesis of PbS nanoparticle including a rapid expansion of supercritical solution (RESS) [6], a solution chemistry [7], a solid-vapor deposition [8] and chemical bath deposition [9]. Since the properties of PbS nanoparticles are highly size-dependent, its properties can be controlled over confined space [10-15]. The developments of numerous methods are available for the synthesis of PbS hybrid, including the reaction between three-dimensional or two-dimensional materials and sodium sulfide ($Na_2S$) [11], [12] or hydrogen sulfide ($H_2S$) [13]-[15], but complex synthesis, time consuming or high reaction temperature may be required for these methods. The formation of PbS clusters smaller than 1.30 nm in the cages of zeolite Y was made by the reaction of $Pb^{2+}$-ion-exchanged zeolite with $Na_2S$ solution followed by the stirring at room temperature for 25 hours [12], while PbS cluster on zeolite A was approached by the explosion of 60 Torr of $H_2S$ for 1 hour [14]. The PbS nanocrystal was synthesized by the reaction between functionalized thiol group-SBA 15 and lead acetate solution subsequent heating at high temperature in $N_2$ atmosphere [10]. The previous report described the preparation of intercalated PbS in the layer and agglomerate PbS on the outer surface of montmorillonite by the reaction between $Pb^{2+}$-montmorillonite and $H_2S$ for 1 hour [15]. Solid-solid reaction is one the most suitable modification techniques of organic-inorganic hybrid materials due to the simple of operation and has been proven a useful technique for the synthesis of nanohybrid materials [16]-[18].

Layered solids, the smectite group of layered clay minerals such as montmorillonite and saponite processes various attractive features such as swelling behavior, large surface area, ion exchange and adsorptive properties for use as a template for nanoparticles [19]. Montmorillonite with 2-dimensional nanospace has been used for confined growth of semiconductor nanoparticles, which lead to a host-guest material with desirable physical properties [20]-[22]. The metal oxide and/or metal selenide nanoparticle of 1.30-10.01 nm were

uniformly distributed between the layers; however, in all cases, the nanoparticles may be located randomly on the external layered surfaces [23]-[26]. We have reported earlier on the *in-situ* formation of metal sulfide-montmorillonite by solid-solid reaction [27]-[29]. In this work, we described a simple facile solid-solid reaction and optical properties of lead sulfide-montmorillonite hybrid.

## 2. Experimental

### 2.1 Materials

Sodium montmorillonite (Kunipia F, Kunimine Industries Co., Ltd., the reference clay sample of the Clay Science Society of Japan, The cation exchange capacity (CEC) is 1.19 meq/1g of clay) was used as a host material. Sodium sulfide ($Na_2S{\cdot}xH_2O$) and lead sulfide ($PbCl_2$) were purchased from Sigma-Aldrich and Carlo Erba Co., Ltd., respectively. All chemicals are analytical grade. All chemical were used without further purification.

### 2.2 Synthesis

Pb(II)-montmorillonite was investigated by conventional ion exchange reaction in which an aqueous suspension of sodium montmorillonite was mixed with an aqueous solution of $PbCl_2$, and the resulting solid was washed repeatedly with deionized water until a negative $AgNO_3$ test was obtained, followed by drying at 40°C for 3 days. The amount of the exchanged lead was 0.98 meq/ 1g of clay. The Pb(II)-montmorillonite-$Na_2S$ hybrid was prepared by the solid-solid reaction as reported previously [29]; the powder of Pb(II)-montmorillonite and $Na_2S{\cdot}xH_2O$ were manually ground with an agate mortar and a pestle at room temperature for 10-15 min. The molar ratio of $S^{2-}$ ion (from $Na_2S{\cdot}xH_2O$) to the Pb(II)-montmorillonite was 1:1.

### 2.3 Characterizations

X-ray diffraction data were recorded on a Bruker D8 ADVANCE diffractometer using monochromatic CuKa radiation. TG-DTA curves were carried out on a Perkin Elmer Pyris Diamond TG-DTA instrument at a heating rate of 10°C/min under a dry air atmosphere using a-alumina (a-$Al_2O_3$) as a standard material. Diffuse reflectance absorption spectra of the solid samples were obtained with a Shimadzu UV-VIS-NIR-3101PC scanning spectrophotometer using an integrated sphere. Photoluminescence spectra were measured on a Shimadzu RF-5301PC spectrofluorophotometer in the wavelength range of 300-900 nm with the excitation at 300 nm.

## 3. Results and Discussion

By the solid-solid reaction of Pb(II)-montmorillonite with $Na_2S{\cdot}xH_2O$ at the molar ratio of 1:1 for Pb(II)-montmorillonite: $S^{2-}$, black powder was obtained. When the hybrid was heated at 200°C the color changed to dark brown. The XRD pattern of

Pb(II)-montmorillonite-$Na_2S$ is shown in **Fig. 1** together with those of Pb(II)-montmorillonite, heat-treated Pb(II)-montmorillonite-$Na_2S$ (200ºC) and $Na_2S$. The Bragg equation relating *d* spacing to scattering angle can be calculated the distance between the layers (basal spacing). The basal spacing ($d_{001}$) of Pb(II)-montmorillonite (**Fig. 1b**) was 1.26 nm associated with the single layer of adsorbed water [30]. After the reaction, the basal spacing of Pb(II)-montmorillonite-$Na_2S$ (**Fig. 1c**) was 1.48 nm was ascribed to the bilayer of adsorbed water [30] and showed the peaks at 26.10, 31.15, 43.26, 51.14, and 53.68 corresponding to the reflection from (111), (200), (220), (311), and (222) planes, respectively, of cubic PbS (JCPDS card number 05-0592) [31]. The XRD pattern of Pb(II)-montmorillonite-$Na_2S$ (**Fig. 1c**) did not show any reflections due to $Na_2S$ crystals (**Fig. 1a**), suggesting that unreacted $Na_2S$ molecule did not remain in the hybrid. The gallery heights of Pb(II)-montmorillonite and Pb(II)-montmorillonite-$Na_2S$ were determined to be 0.30 and 0.52 nm (**Table 1**) by subtracting the thickness of silicate layer (0.96 nm) from the observed basal spacing. The gallery height of Pb(II)-montmorillonite-$Na_2S$ is probably the consequence of the intercalation of $S^{2-}$ (0.36 nm in diameter) because the gallery height (0.52 nm) is large to intercalate $S^{2-}$ and subsequent *in-situ* formation of lead sulfide in the layers. The appearance of the reflection due to cubic PbS in the XRD pattern of Pb(II)-montmorillonite-$Na_2S$ was ascribed to the formation of PbS crystal on the outer surface of montmorillonite. Pb(II)-montmorillonite-$Na_2S$ was heated at 200ºC for 1 hour in air atmosphere, the basal spacing of the heat-treated Pb(II)-montmorillonite-$Na_2S$ was decreased to 1.20 nm (**Fig. 1d**), corresponding to the gallery height 0.24 nm, suggesting to the dehydration, and the diffraction peaks due to cubic PbS crystal were detected. According to the gallery height of the heat-treated Pb(II)-montmorillonite-$Na_2S$ indicated the formation of lead sulfide particle in the interlayer space of montmorillonite with a height of ca. 0.24 nm and the lead sulfide particle was thought to be lying flat between the layers.

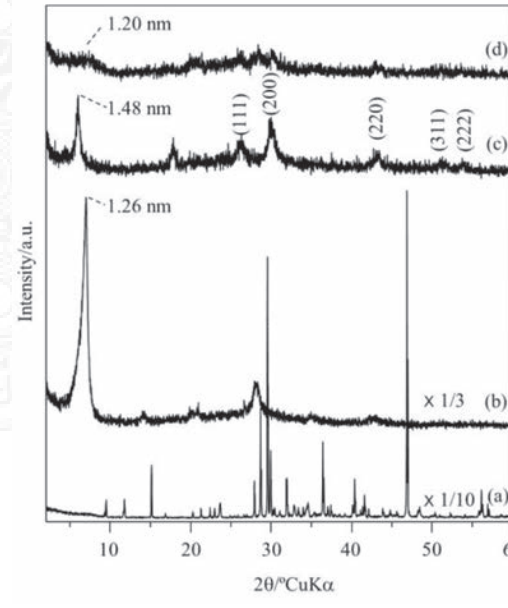


**Fig. 1** X-ray diffraction patterns of (a) $Na_2S$, (b) Pb(II)-montmorillonite, (c) Pb(II)-montmorillonite-$Na_2S$, (d) heat-treated Pb(II)-montmorillonite-$Na_2S$ (200ºC)

**Table 1** The basal spacing ($d_{001}$) and gallery height of products

| Sample | Basal spacing/ nm | Gallery height/nm |
|---|---|---|
| Pb(II)-montmorillonite | 1.26 | 0.30 |
| Pb(II)-montmorillonite-$Na_2S$ | 1.48 | 0.52 |
| Heat-treated Pb(II)-montmorillonite-$Na_2S$ | 1.20 | 0.24 |

The TG-DTA curves of Pb(II)-montmorillonite-$Na_2S$ are shown in **Fig. 2** together with those of Pb(II)-montmorillonite and $Na_2S$. The TG curve of Pb(II)-montmorillonite (**Fig. 2a**) showed three steps of weight loss. The initial weight loss was observed at room temperature to 200ºC which corresponding the endothermic peaks at 69ºC and 170ºC (**Fig. 2d**), was ascribed to dehydration. The water content at this temperature is determined to be 12.92%. The second weight loss observed at the temperature range of 200-550ºC, indicating the dehydration of retained water associated with 2.36% of water content. The last weight loss between 550 and 800ºC without significant endothermic or exothermic peak in the DTA curve was interpreted to the dehydroxylation due to the collapse of the hydroxyl group of montmorillonite [32]. The TG curve of Pb(II)-montmorillonite-$Na_2S$ (**Fig. 2b**) showed three steps of weight loss. The first weight loss from room temperature to 200ºC which corresponding to the endothermic peak at 72ºC (**Fig. 2e**) suggesting to the dehydration of water with 39.54% of water content. The water content in Pb(II)-montmorillonite-$Na_2S$ was comparable to Pb(II)-montmorillonite, the increase in the water content might be a consequent of adsorption of water molecules during the solid-solid reaction at room temperature. The second weight loss from 200 to 550ºC corresponding to 6.62% of remained water content. The last weight loss between 550 and 845ºC without significant endothermic or exothermic peak in the DTA curve was interpreted to the dehydroxylation of montmorillonite and the melting of PbS [32], [33]. It has been reported that the weight loss in the range of 660-820ºC corresponding to the endothermic peak at 762ºC was assigned to PbS melting [33]. The TG curve of $Na_2S$ (**Fig. 2c**) showed the weight loss from room temperature to 300ºC corresponding to the endothermic peaks at 52, 91 and 194ºC (**Fig. 2f**), suggesting to the melting and vaporization of $Na_2S$. The endothermic peaks at 52, 91 and 194ºC were absent in the DTA curve of Pb(II)-montmorillonite-$Na_2S$ (**Fig. 2e**), implying that the hybrid did not contain unreacted $Na_2S$.

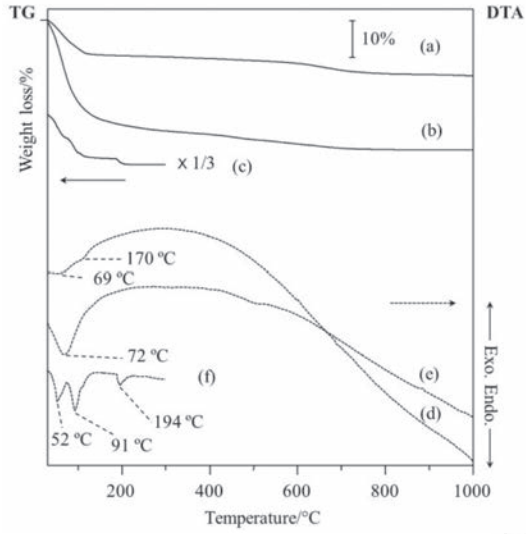


**Fig. 2** TG-DTA curves of (a, d) Pb(II)-montmorillonite, (b,e) Pb(II)-montmorillonite-$Na_2S$, (c, f) $Na_2S$

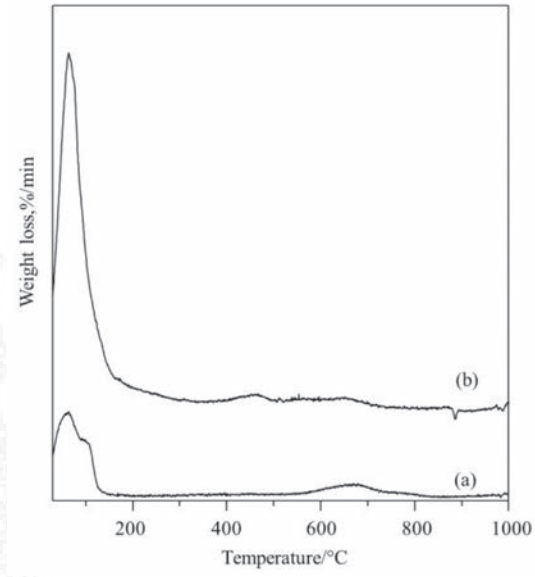


**Fig. 3** DTG curves of (a) Pb(II) montmorillonite-$Na_2S$, (b) Pb(II) montmorillonite

The difference in the TG curve of the last weight loss was further confirmed by the DTG curve (**Fig. 3**). In the DTG curve of Pb(II)-montmorillonite-$Na_2S$ (**Fig. 3a**), the last weight loss between 550 and 845°C showed two processes, indicating the dehydroxylation of montmorillonite and melting of PbS [32], [33] while the last weight loss between 550-800°C in DTG curve of Pb(II)-montmorillonite (**Fig. 3b**) showed only one process due to dehydroxylation of montmorillonite [32].

UV-Vis diffuse reflectance spectra of the hybrids are shown in **Fig. 4**. Nanosized semiconductor particles generally exhibited the blue shifted of the absorption onset with decreasing particle size [1]. The non-resolved absorption bands at 298 and 328 nm were seen in absorption spectra of Pb(II)-montmorillonite-$Na_2S$ (**Fig. 4c**) and heat-treated Pb(II)-montmorillonite-$Na_2S$ (**Fig. 4d**), respectively. It can be seen that the obtained absorption onsets at 414 and 508 nm of Pb(II)-montmorillonite-$Na_2S$ (**Fig. 4c**) and heat-treated Pb(II)-montmorillonite-$Na_2S$ (**Fig. 4d**), respectively, were dramatic blue-shifted from the absorption onset of the bulk PbS (3020 nm) [3]. The band gaps were calculated to be 1.83 and 1.50

eV for Pb(II)-montmorillonite-$Na_2S$ and heat-treated Pb(II)-montmorillonite-$Na_2S$, respectively. The formation of PbS in the cages of zeolite Y with the particle sizes vary between 0.56-1.20 nm showed the absorption peaks and absorption onsets in the range 292-308 and 324-337 nm, respectively [12]. The absorption bands of the hybrids (298 and 328 nm) were near the absorption band of PbS in zeolite Y, make us believed that PbS particles with ca. 0.24 nm-thick were immobilized in the interlayer spaces of montmorillonite. A shift of the absorption onset of Pb(II)-montmorillonite-$Na_2S$ (414 nm) towards higher wavelength of heat-treated Pb(II)-montmorillonite-$Na_2S$ (508 nm) was attributed to the increasing of PbS nanoparticles size. The PbS-polyvinylalcohol (PVA) nanoparticles displayed three well-defined absorption peaks, exciton absorption peak, around 300, 400 and 600 nm ascribed to the $1S_e$-$1S_h$, $1S_e$-$1P_h$, and $1P_e$-$1P_h$, transitions, respectively [34]. In spite of the PbS nanoparticles having a size in the confinement space of montmorillonite, their absorption spectra did not display the excitonic absorption peak, instead of, it is observed absorption bands at about 298, 328 for Pb(II)-montmorillonite-$Na_2S$ and heat-treated Pb(II)-montmorillonite-$Na_2S$, respectively. The lack of excitonic structure in the absorption spectra of PbS nanoparticles was attributed to the broad particle size distribution and/or oxygen defect on the surface of PbS nanoparticles [13]. In addition, the absorption shoulders were observed at 603 and 627 for Pb(II)-montmorillonite-$Na_2S$ and heat-treated Pb(II)-montmorillonite-$Na_2S$,respectively indicating to the adsorbed PbS on the outer surface or edge of the layer.

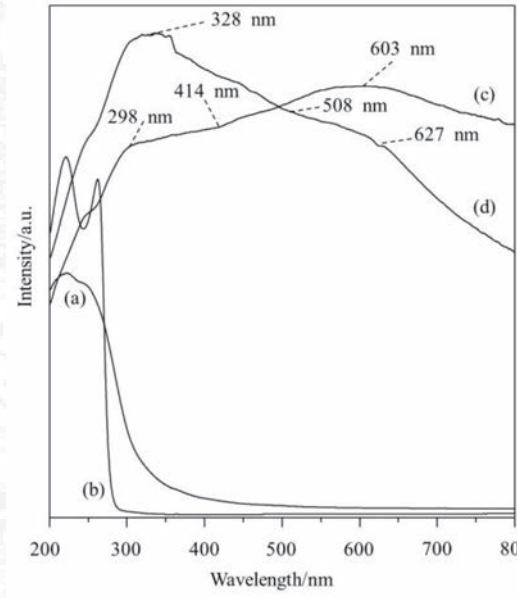


**Fig. 4** Diffuse reflectance absorption spectra of (a) Pb(II)-montmorillonite, (b) $Na_2S$, (c) Pb(II)-montmorillonite-$Na_2S$, (d) heat-treated Pb(II)-montmorillonite-$Na_2S$

In previous publications, we reported the synthesis and optical properties of semiconductor-montmorillonite [27]. We found that the nanosize metal sulfide with the exciton Bohr radius between 2.5-2.8 nm such as CdS or ZnS can be immobilized in the interlayer spaces of montmorillonite by the solid-solid

reaction. However, both species, including immobilized and adsorbed PbS was observed, which can be ascribed to the large exciton Bohr radius of PbS (18 nm).

The photoluminescence spectra of the hybrids are shown in **Fig. 5**. The photoluminescence spectrum of Pb(II)-montmorillonite-$Na_2S$ did not show emission peak (**Fig. 5a**). In the photoluminescence spectrum of heat-treated Pb(II)-montmorillonite-$Na_2S$, the emission peak was observed at 367 nm (**Fig. 5b**). The photoluminescence spectra showed many position peaks if the host or surrounding of the PbS particle were different matrix materials [14]. PbS monomer in zeolite A showed the emission peak at 568 nm [14] but not detected for the PbS in zeolite Y [12]. The PbS nanoparticles embedded in sol-gel silica glass showed two emission peaks at 440 and 605 nm [35]. Therefore the observed emission peak of 367 nm can be ascribed to the emission of PbS nanoparticle. The distinguish two kinds of surface states are deep states and shallow surface states [36]. The photoluminescence emission peak (at 367 nm) was found in the near non-resolve absorption band at 328 for heat-treated Pb(II)-montmorillonite-$Na_2S$ was assigned mainly to a shallow trap states. The luminescence property of PbS particle can be affected by a host material. It has been reported that the luminescence intensity of PbS was efficiently quenched by the presence of water because water acts as a trap site for the exciton, which can deactivate the excited state by non-radiative decay [37]. The observed emission peak of heat-treated Pb(II)-montmorillonite-$Na_2S$ (at 367 nm) can be attributed to the removal of adsorbed water. The information from thermogravimetric analysis (TGA) was correlated to the luminescence intensity of the hybrids measured at room temperature and heat-treatment at 200°C. The low luminescence intensity of the hybrid can be ascribed to the quenching of iron, which is an impurity in montmorillonite [19].

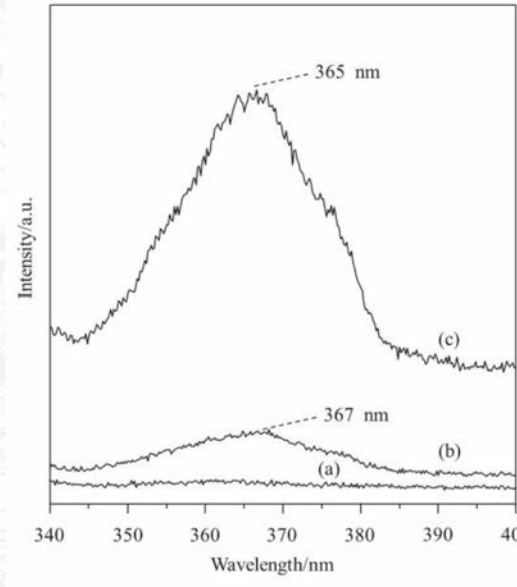


**Fig. 5** Photoluminescence spectra of (a) Pb(II)-montmorillonite-$Na_2S$, (b) heat-treated Pb(II)-montmorillonite-$Na_2S$, (c) Colloidal PbS

The immobilized and/or adsorbed PbS nanoparticles was removed from montmorillonite by stirred heat-treated Pb(II)-montmorillonite-$Na_2S$ in absolute

ethanol for 1 hour followed by the centrifugation at 4,000 rpm. The emission peak of colloid PbS showed at 365 nm (**Fig. 5c**). The colloid PbS showed two emission peaks at 510 and 627 nm [38]. The emission intensity of colloid PbS at 365 nm increased 5.74 times than the emission peak at 367 nm of the heat-treated Pb(II)-montmorillonite-$Na_2S$. By comparison with the conventional reaction, the reaction between $PbCl_2$ and $Na_2S \cdot xH_2O$ at room temperature was synthesized. It was found that PbS get precipitated after 15 minutes. No detectable of the emission signal was observed for the powder and supernatant samples. Montmorillonite is a potential layer for use as a template for PbS colloidal.

## 4. Conclusion

The hybrid of lead sulfide and montmorillonite was prepared by solid-solid reaction between lead exchanged ion in montmorillonite and sodium sulfide. The UV-Vis absorption and photoluminescence spectra confirmed the formation of lead sulfide (PbS) on montmorillonite. The removal water from lead sulfide particle can significantly enhance luminescence intensity. The available work shows that solid-solid reaction is a simple, less time consuming, economic and efficient method for the preparation of hybrid material.

## 5. Acknowledgment

The authors gratefully acknowledge the Rajamangala University of Technology Isan, Nakhon Ratchasima for all supports and liberality.

## 6. References

[1] K. Rajeshwar, N. R. de Tacconi and C. R. Chenthamarakshan, "Semiconductor-based composite materials: preparation, properties, and performance," *Chemistry of Materials*, vol. 13, pp. 2765-2782, 2001.

[2] T. Trindade, "Nanocrystalline semiconductors: synthesis, properties, and perspectives," *Chemistry of Materials*, vol. 13, pp. 3843-3858, 2001.

[3] T. K. Singh and S. K. Sharma, "Lead sulphide-doped silica xerogel by sol-gel technique," *Defence Science Journal*, vol. 46, pp. 105-107, 1996.

[4] J. Li and J. Z. Zhang, "Optical properties and applications of hybrid semiconductor nanocrystals," *Coordination Chemistry Reviews*, vol. 253, pp. 3015-3041, 2009.

[5] A. P. Alivisatos, "Perspectives on the physical chemistry of semiconductor nanocrystals," *Journal of Physical Chemistry*, vol. 100, pp. 13226-13239, 1996.

[6] Y. -P. Sun, R. Guduru, F. Lin and T. Whiteside, "Preparation of nanoscale semiconductors through the rapid expansion of supercritical solution (RESS) into liquid solution," *Industrial*

*and Engineering Chemistry Research,* vol. 39, pp. 4663-4669, 2000.

[7] S. Chen, L. A. Truax and J. M. Sommers, "Alkanethiolate-protected PbS nanoclusters: synthesis, spectroscopic and electrochemical studies," *Chemistry of Materials*, vol. 12, pp. 3864-3870, 2000.

[8] A. S. Obaid, M. A. Mahdi and Z. Hassan, "Growth of nanocrystalline PbS thin films by solid-vapor deposition," *Advanced Materials Research,* vol. 620, pp. 1-6, 2013.

[9] S. Seghaier, N. Kamoun, R. Brini and A.B. Amara, "Structural and optical properties of PbS thin films deposited by chemical bath deposition," *Materials Chemistry and Physics,* vol. 97, pp. 71-80, 2006.

[10] F. Gao, Q. Lu, X. Liu, Y. Yan and D. Zhao, "Controlled synthesis of semiconductor PbS nanocrystals and nanowires inside mesoporous silica SBA-15 phase," *Nano Letter*s, vol. 1, pp. 743-748, 2001.

[11] M. Flores-Acosta, M. Sotelo-Lerma, H. Arizpe-Chávez, F. F. Castillón-Barraza and R. Ramírez-Bon, "Excitonic absorption of spherical PbS nanoparticles in zeolite A," *Solid State Communication*s, vol. 128, pp. 407-411, 2003.

[12] W. Chen, Z. Wang, Z. Lin, J. Qian and L. Lin, "New observation on the formation of PbS clusters in zeolite-Y," *Applied Physics Letters,* vol. 68, pp. 1990-1992, 1996.

[13] K. Moller, T. Bein, N. Herron, W. Mahler and Y. Wang, "Encapsulation of lead sulfide molecular clusters into solid matrices, structural analysis with X-ray absorption spectroscopy," *Inorganic Chemistry,* vol. 28, pp. 2914-2919, 1989.

[14] C. Leiggener and G. Calzaferri, "Synthesis and luminescence properties of $Ag_2S$ and PbS clusters in zeolite A," *Chemistry A European Journal*, vol. 11, pp. 7191-7198, 2005.

[15] L. Jankovič, K. Dimos, J. Bujdk, I. Koutselas, J. Madejová, D. Gournis, M.A. Karakassides and P. Komadel, Synthesis and characterization of low dimensional ZnS- and PbS-semiconductor particles on montmorillonite template," *Physical Chemistry Chemical Physics.*, vol. 12, pp. 14236-14244, 2010.

[16] M. Ogawa, T. Kuroda and K. Kato, "Intercalation of 2,2¢-bipyridine and complex formation in the interlayer space of montmorillonite by solid-solid reactions," *Inorganic Chemistry,* vol. 30, pp. 584-585, 1991.

[17] M. Ogawa, Y. Nagafusa, K. Kuroda and C. Kato, "Solid-state intercalation of crylamide into smectites and Na-taeniolite," *Applied Clay Science,* vol. 7, pp. 291-302, 1992.

[18] M. Ogawa, T. Aono, K. Kuroda and C. Kato, "Photophysical probe study of alkylammonium-montmorillonites." *Langmuir,* vol. 9,

pp. 1529-1533, 1993.

[19] M. Ogawa, K. Saito and M. Sohmiya, "A controlled spatial distribution of functional units in the two dimensional nanospace of layered silicates and titanates," *Dalton Trans*, vol. 43, pp. 10340-10354, 2014.

[20] S. Miao, Z. Liu, B. Han, H. Yang, Z. Miao and Z. Sun, "Synthesis and characterization of ZnS-montmorillonite nanocomposites and their application for degrading eosin B," *Journal of Colloid and Interface Science*, vol. 301, pp. 116-122, 2006.

[21] C. Ooka, S. Akita, Y. Ohashi, T. Horiuchi, K. Sukuki, S.-I. Komai, H. Yoshida and T. Hattori, "Crystallization of hydrothermally treated $TiO_2$ pillars in pillared montmorillonite for improvement of the photocatalytic activity," *Journal of Materials Chemistry*, vol. 9, pp. 2943-2952, 1999.

[22] Z. Han, H. Zhu, S. R. Bulcock and S.P. Ringer, "One-step synthesis and structural features of CdS/montmorillonite nanocomposites," *Journal of Physic Chemistry B*, vol. 109, pp. 2673-2678, 2005.

[23] N. Khaorapapong, N. Khumchoo and M. Ogawa, "Preparation of zinc oxide-montmorillonite hybrids," *Materials Letters*, vol. 65, pp. 657-660, 2011.

[24] N. Khaorapapong, N. Khumchoo and M. Ogawa, "Preparation of copper oxide in smectites," *Applied Clay Science*, vol. 104, pp. 238-244, 2015.

[25] A. Ontam, N. Khaorapapong and M. Ogawa, "An incorporation of cadmium selenide at organophilic surface of clay mineral," *Colloids and Surfaces A: Physicochemical and Engineering Aspects*, vol. 411, pp. 27-33, 2012.

[26] A. Ontam, N. Khaorapapong and M. Ogawa, "Immobilization of cadmium telluride nanoparticles on the surface of hexadecyltrimethylammonium-montmorillonite," *Journal of Materials Chemistry*, vol. 22, pp. 20001-20007, 2012.

[27] N. Khaorapapong, A. Ontam, S. Yongme and M. Ogawa, "Solid-state intercalation and *in situ* formation of cadmium sulfide in the interlayer space of montmorillonite," *Journal of Physics and Chemistry of Solids*, vol. 69, pp. 1107-1111, 2008.

[28] N. Khaorapapong, A. Ontam, J. Khemprasit and M. Ogawa, "Formation of MnS- and NiS-montmorillonites by solid-solid reactions," *Applied Clay Science*, vol. 43, pp. 238-242, 2009.

[29] N. Khaorapapong, A. Ontam and M. Ogawa, "Very slow formation of copper sulfide and cobalt sulfide nanoparticles in montmorillonite," *Applied Clay Science*, vol. 51, pp. 182-186, 2011.

[30] D. M. Clementz, T. J. Pinnavain and M. M. Mortland, "Stereochemistry

of hydrate copper(II) ions on the interlamellar surface of layer silicates. An electron spin resonance study," *Journal Physic Chemistry B*, vol. 101, pp. 7786-7793, 1973.

[31] N. M. Huang, S. Radiman, H. N. Lim, S. K. Yeong, P. S. Khiew, W. S. Chiu, S. N. Kong and G. H. Mohamed Saeed. "Synthesis and characterization of ultra small PbS nanorods in sucrose ester microemulsion," *Materials Letters*, vol. 63, pp. 500-503, 2009.

[32] S. Guggenheim and A. F. K. van Groos. "Baseline studies of the clay minerals society source clays: thermal analysis," *Clays and Clay Minerals*, vol. 49, pp. 433-443, 2001.

[33] T. S. Shyju, S. Anandhi, R. Sivakumar and R. Gopalakrishnan. "Studies on lead sulfide (PbS) semiconducting thin films deposited from nanoparticles and its NLO application," *International Journal of Nanoscience*, vol. 13, pp. 1450001-1450013, 2014.

[34] L. Guo, K. Ibrahim, F. Q. Liu, X. C. Ai, Q. S. Li, H. S. Zhu and Y. H. Zou. "Transient optical properties of novel PbS nanoparticles coated with 2,6-O-diallyl-b-CD," *Journal of Luminescence*, vol. 82, pp. 111-114, 1999.

[35] P. Yang, C. F. Song, M. K. Lü, X. Yin, G. J. Zhou, D. Xu and D. R. Yuan, "The luminescence of PbS nanoparticles embedded in sol-gel silica glass," *Chemical Physics Letters*, vol. 345, pp. 429-434, 2001.

[36] A. Martucci, J. Fick, S.-É. LeBlanc, M. LoCascio and A. Haché, "Optical properties of PbS quantum dot doped sol-gel films," *Journal of Non-Crystalline solids*, vol. 345, pp. 639-642, 2004.

[37] S. W. Buckner, R. L. Konold and P. A. Jelliss, "Luminescence quenching in PbS nanoparticles," *Chemical Physics Letters*, vol. 394, pp. 400-404, 2004.

[38] M. S. Ghamsari, M. H. M. Ara, S. Radiman and X. H. Zhang, "Colloidal lead sulfide nanocrystals with strong green emission," *Journal of Luminescence*, vol. 137, pp. 241-244, 2013.